Electronic Supplementary Material (ESI) for Lab on a Chip.

Supplementary Information

Simultaneous metering and dispensing of multiple reagents on passively controlled microdevice solely by finger pressing

Kerui Xu[1], Matthew R. Begley[2,3] and James P. Landers[1,4,5*]

[1]Department of Chemistry, University of Virginia, Charlottesville, VA 22904, USA
[2]Department of Mechanical Engineering,[3]Materials Department,
University of California Santa Barbara, Santa Barbara, CA 93106, USA
Departments of [4]Mechanical and Aerospace Engineering, [5]Pathology
University of Virginia, Charlottesville, VA 22904, USA

1. Fabrication of Glass-PDMS-glass (GPG) fluidic diode

In order to control the depth of laser ablation in PDMS, both the scan speed and power of the CO_2 laser were adjusted[1]. We maintained a constant laser scan speed and varied the power in order to achieve an ablation depth that fully covered the thickness of PDMS film (Fig. S1). The floor and wall of the ablated channels were rough compared with that of cured PDMS using an SU-8 mold. This is, however, of no consequence to the bonding and performance of the diode, because only the non-ablated outer PDMS surfaces will be in contact with glass valve seat and cover plate. The trapezoid-shaped cross-sectional view of the channels with a width gradient at the channel edge was consistent with the cone-shaped cross-sectional view of CO_2 laser cutting line[2]. This indicates that the Gaussian-shape of the focused laser beam and the width expansion of ~75 μm on each side at the top of the cone defines the spatial resolution of laser ablation. At a fixed scan speed, the ablation depth in the PDMS film is linear with respect to laser power. The linear

relationship between depth and power is consistent with previously reported work[1], [2] and the linear profile implies that the depth of ablation can easily be controlled by simply adjusting the power input of laser ablation. The engraving depth has an average around 2% RSD. In addition to the ablation uncertainties, the final thickness of the flap is also dependent on the initial thickness of the intact film, in order not to add significant variance to the final thickness of the flap, the thicknesses of all the films we used were controlled at 290 (±2) µm by measuring prior to the fabrication. The fluidic diode we used in our microdevice has a PDMS flap that was 60 µm thick by engraving down 230 µm in the commercialized film, and the final thickness of the flap has ~ 10% variation.

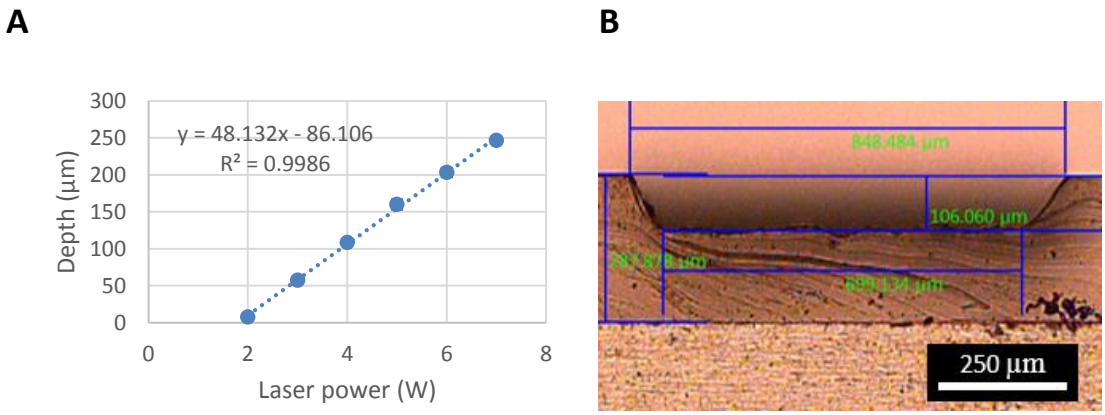

Figure S1. Laser ablation in PDMS film. (A) engraving depth of laser ablation in PDMS versus laser power (n=6). (B) cross-sectional views of laser-engraved PDMS channel at laser power = 4W.

2. Determination of open pressure

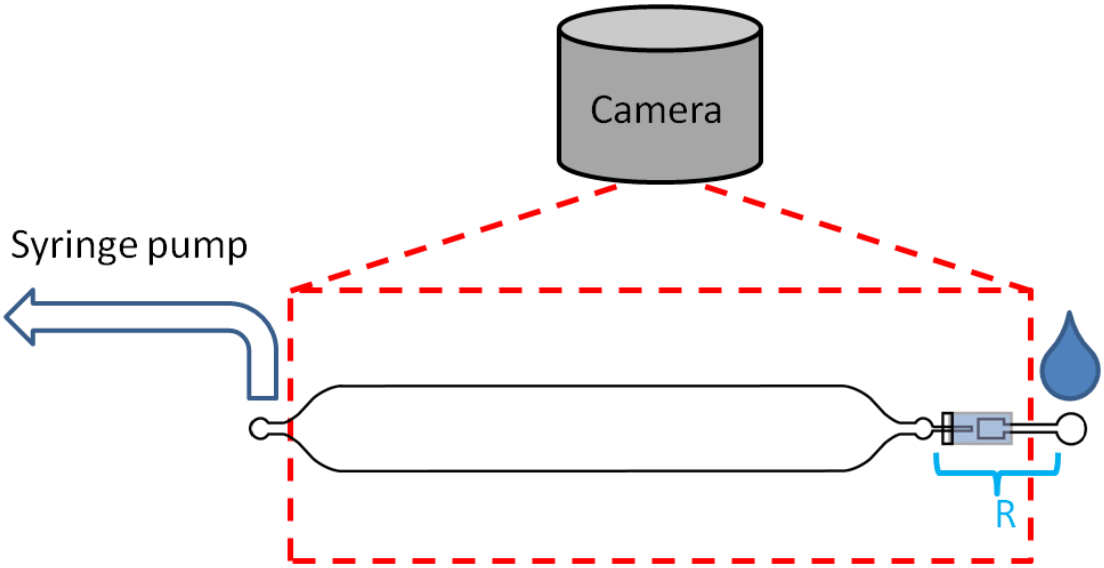

Figure S2, settings for open pressure and flow profile determination

The flow chamber and connection set-up is shown in Figure S2. A fluidic diode is located in between the inlet reservoir and flow chamber. Initially a drop of Erioglaucine solution is placed in the inlet reservoir and then we start drawing by a syringe pump at fixed flow rate. The inner pressure p changes as the syringe progresses with following relation:

$$p(t) = p_0 \frac{V_0}{V_0 + V(t)} = p_0 \frac{V_0}{V_0 + qt} \quad (1)$$

wherein V_0 is the initial total volume of the system and V is the volume that has been drawn into the syringe on time point t at fixed flow rate q. p0 is the initial inner pressure (1 atm).

At closed state, the pressure difference across the fluidic diode is:

$$\Delta p = p_0 - p(t) \quad (2)$$

When Δp is over the open pressure threshold p_{open}, solution begins to flow in and we stop the syringe pump immediately. After that point, the inner pressure changes as:

$$(t) = p_0 \frac{V_0}{V_0 + V1 - V'(t)} \quad (3)$$

wherein V_1 is the volume that has been drawn into the syringe when it stops, and V'(t) is the volume of liquid that has flown into the chamber and can be determined from the video at each time point.

The overall resistance of the liquid flowing is then calculated as:

$$R = \frac{\frac{dV'(t)}{dt}}{p(t)} \quad (4)$$

where $\frac{dV'(t)}{dt}$ is determined from the plot of V'(t) versus t. Because the resistance of flow chamber and the air-filled downstream channel are much smaller than that of the liquid filled connecting channel and diode, the measured resistance is dominated by the incoming channel and diode (Fig. S2). We minimized the incoming channel's resistance so that the resistance change of the diode versus pressure can be shown in the overall resistance profile.

3. Mixing ratio determination and reagent components in STR PCR

Table S1 *Essential reagents in AmpFLSTR® Identifiler® PCR Amplification Kit and their optimal volumes (unit: μL)*

	Taq Gold Polymerase	Reaction mix	Dnase free diH_2O	Standard DNA (or sample DNA)
Volume needed per run in a tube	0.45	5	9.5	10
Dispensed volume per MaD cycle	0.15	1.65	3.2	3.3

To determine the volume of each dye solution in the mixture, an extinction coefficient matrix is used[3]

$$\begin{bmatrix} \varepsilon_{t,\lambda1,}b & \varepsilon_{a,\lambda1,}b & \varepsilon_{e,\lambda1,}b & \varepsilon_{T,\lambda1,}b \\ \varepsilon_{t,\lambda2,}b & \varepsilon_{a,\lambda2,}b & \varepsilon_{e,\lambda2,}b & \varepsilon_{T,\lambda2,}b \\ \varepsilon_{t,\lambda3,}b & \varepsilon_{a,\lambda3,}b & \varepsilon_{e,\lambda3,}b & \varepsilon_{T,\lambda3,}b \\ \varepsilon_{t,\lambda4,}b & \varepsilon_{a,\lambda4,}b & \varepsilon_{e,\lambda4,}b & \varepsilon_{T,\lambda4,}b \end{bmatrix} \begin{bmatrix} c_t \\ c_a \\ c_e \\ c_T \end{bmatrix} = \begin{bmatrix} A_{\lambda1} \\ A_{\lambda2} \\ A_{\lambda3} \\ A_{\lambda4} \end{bmatrix} \quad (5)$$

or

$$\begin{bmatrix} \varepsilon_{t,\lambda1,}b & \varepsilon_{a,\lambda1,}b & \varepsilon_{e,\lambda1,}b & \varepsilon_{T,\lambda1,}b \\ \varepsilon_{t,\lambda2,}b & \varepsilon_{a,\lambda2,}b & \varepsilon_{e,\lambda2,}b & \varepsilon_{T,\lambda2,}b \\ \varepsilon_{t,\lambda3,}b & \varepsilon_{a,\lambda3,}b & \varepsilon_{e,\lambda3,}b & \varepsilon_{T,\lambda3,}b \\ \varepsilon_{t,\lambda4,}b & \varepsilon_{a,\lambda4,}b & \varepsilon_{e,\lambda4,}b & \varepsilon_{T,\lambda4,}b \end{bmatrix} \begin{bmatrix} c_{t0}V_{tx}/V \\ c_{a0}V_{ax}/V \\ c_{e0}V_{ex}/V \\ c_{T0}V_{Tx}/V \end{bmatrix} = \begin{bmatrix} A_{\lambda1} \\ A_{\lambda2} \\ A_{\lambda3} \\ A_{\lambda4} \end{bmatrix} \quad (6)$$

To minimize the overlapping of the spectra of different dye solutions we only used 3 types of dye and the fourth reagent is TE buffer. However, because TE buffer is transparent so the last column of the coefficient matrix is zero and this set of simultaneous equations doesn't have a definite solution. By drawing and diluting a 5 μL aliquot of MaD-ed mixture rather than all of it, we introduce another linearly independent equation into this equation set:

$$\begin{bmatrix} \varepsilon_{t,\lambda1,}b & \varepsilon_{a,\lambda1,}b & \varepsilon_{e,\lambda1,}b & \varepsilon_{T,\lambda1,}b \\ \varepsilon_{t,\lambda2,}b & \varepsilon_{a,\lambda2,}b & \varepsilon_{e,\lambda2,}b & \varepsilon_{T,\lambda2,}b \\ \varepsilon_{t,\lambda3,}b & \varepsilon_{a,\lambda3,}b & \varepsilon_{e,\lambda3,}b & \varepsilon_{T,\lambda3,}b \\ V/c_{t0} & V/c_{a0} & V/c_{e0} & V/c_{T0} \end{bmatrix} \begin{bmatrix} c_{t0}V_{tx}/V \\ c_{a0}V_{ax}/V \\ c_{e0}V_{ex}/V \\ c_{T0}V_{Tx}/V \end{bmatrix} = \begin{bmatrix} A_{\lambda1} \\ A_{\lambda2} \\ A_{\lambda3} \\ V_{aliquot} \end{bmatrix} \quad (7)$$

By doing so this set of equations has a definite solution and all volumes can be determined given a mixture's spectrum as well as all parameters.

4. Protein quantitation using CBBG

CBBG-protein solution was incubated for 1 min and then the scanned raw image (Fig. S3A, upper panel) was converted to into HSB space (Hue, Saturation and Brightness)(Fig. S3A, lower panel). The saturation value in unit of grayscale is measured and correlated with protein concentration, using water as background (Fig. S3B).

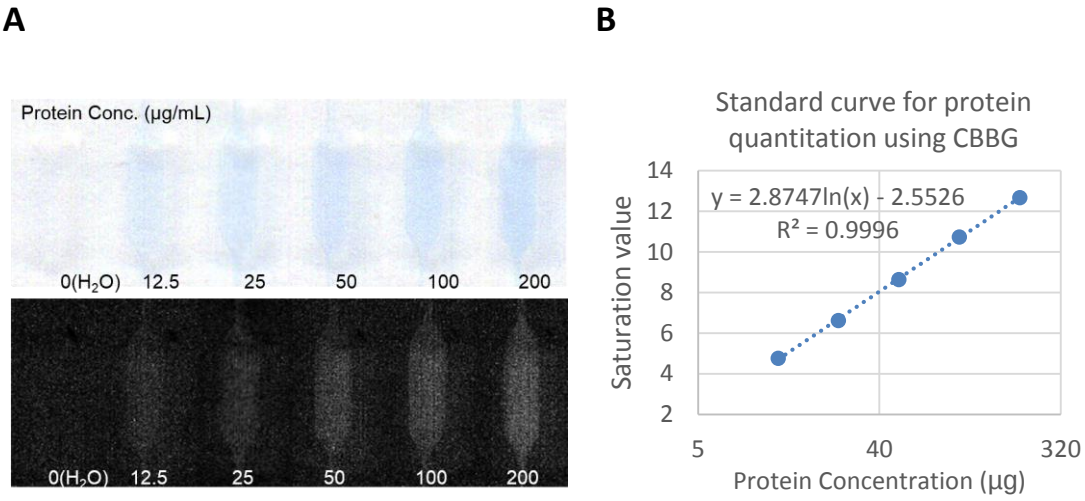

Figure S3. Protein quantitation using CBBG. **A.** Images of CBBG-protein solution in RGB space (upper) and in the Saturation channel of HSB space (lower); **B.** The standard curve of protein quantitation using CBBG.

Reference

[1] B. A. Fogarty, K. E. Heppert, T. J. Cory, K. R. Hulbutta, R. S. Martin, and S. M. Lunte, "Rapid fabrication of poly(dimethylsiloxane)-based microchip capillary electrophoresis devices using CO_2 laser ablation.," *Analyst*, vol. 130, no. 6, pp. 924–30, Jun. 2005.

[2] H.-B. Liu and H.-Q. Gong, "Templateless prototyping of polydimethylsiloxane microfluidic structures using a pulsed CO_2 laser," *J. Micromechanics Microengineering*, vol. 19, no. 3, Mar. 2009.

[3] D. C. Leslie, B. a. Melnikoff, D. J. Marchiarullo, D. R. Cash, J. P. Ferrance, and J. P. Landers, "A simple method for the evaluation of microfluidic architecture using flow quantitation via a multiplexed fluidic resistance measurement," *Lab Chip*, vol. 10, no. 15, p. 1960, 2010.